ACS OMEGA

Article

http://pubs.acs.org/journal/acsodf

Humic Acid as a Sensitizer in Highly Stable Dye Solar Cells: Energy from an Abundant Natural Polymer Soil Component

Rohit L. Vekariya,[†,‡] Keval K. Sonigara,[†] Kishan B. Fadadu,[†] Jayraj V. Vaghasiya,[†] and Saurabh S. Soni*[,†]

[†]Department of Chemistry, Sardar Patel University, Vallabh Vidyanagar, Anand 388 120, Gujarat, India

[‡]School of Chemical Engineering, Fuzhou University, Fuzhou 350116, Fujian Province, P. R. China

Supporting Information

ABSTRACT: Humic acid (HA), a natural polymer and soil component, was explored as a photosensitizer in dye-sensitized solar cells (DSSCs). Photophysical and electrochemical properties show that HA covers a broad visible range of the electromagnetic spectrum and exhibits a quasi-reversible nature in cyclic voltammetry (CV). Because of its abundant functionalities, HA was able to bind onto the nano-titania surface and possessed good thermal stability. HA was employed as a sensitizer in DSSCs and characterized by various photovoltaic techniques such as *I*−*V*, incident-photo-to-current conversion efficiency (IPCE), electrochemical impedance spectroscopy (EIS), and Tafel polarization. The HA-based device shows a power conversion efficiency (PCE) of 1.4% under 1 sun illumination. The device performance was enhanced when a coadsorbent, chenodeoxycholic acid (CDCA), along with HA was used and displayed 2.4% PCE under 0.5 sun illumination. The DSSCs employing HA with CDCA showed excellent stability up to 1000 h. The reported efficiency of devices with HA is better than that of devices with all natural sensitizers reported so far.

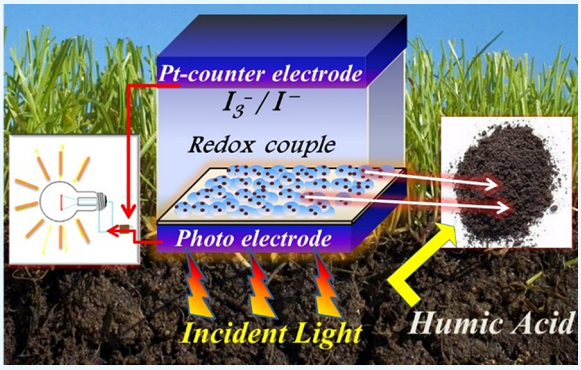

INTRODUCTION

Dye-sensitized solar cells (DSSCs), regarded as one of the most promising classes of photovoltaic devices, have been extensively investigated because of their high theoretical efficiency, facile fabrication process, and low cost.[1] Commonly, the major components of DSSCs are photoelectrodes, sensitizers, electrolytes, and counter electrodes. Among these four major components, sensitizers definitely play an important role as they are the origin of light harvesting in dye solar cells. DSSCs exhibit a power conversion efficiency (PCE) up to 13% by exploiting a porphyrine sensitizer and graphene nanoplatelets as a counter electrode.[2,3] Metal-based organic sensitizers such as ruthenium,[4] osmium[5] polypyridin complexes, and D−π−A metal free organic dyes[6,7] have been used extensively as efficient sensitizers. Synthesis routes of these sensitizers are often composed of multistep processes followed by long, hard, and costly chromatographic separation for purification. All of these lead to the production of a large amount of synthetic waste, which has a bad impact on the environment. In front of these sensitizer categories, natural sensitizers and their derivatives are pronounced candidates for environmentally friendly DSSCs because they are nontoxic, low in cost, renewable, and abundant in nature. Additionally, because of simple and cheap chemical/physical processing, natural materials do not produce any hazardous byproducts. Thus, some natural resources such as natural dyes have been investigated to convert solar energy into electricity.[8,9] These natural dyes are extracted from vegetables, flowers, fruits, leaves, algae, etc., and they are able to generate PCE between 0.01 and 1.7%.[10] Low power conversion and instability are also the crucial weak factors of natural dyes.

In view of this, we are introducing a naturally abundant polymer, humic acid (HA) (Scheme 1), as a sensitizer in dye solar cells, which can be extracted from soil, wood, coal, or seawater.[11,12] Soil has a very versatile chemical composition, comprising thousands of organic as well as inorganic elements. It contains a lot of essential metallic as well as nonmetallic elements which are explored for their applications in a variety of fields.[13] One of the key components of soil is HA, which is believed to be a product of transformation of organic compounds. It may be defined as a mixture of high-molecular-weight macromolecules (0.500−100k Da) of natural origin.[14] A typical HA molecule contains aromatic rings and aliphatic chains that host numerous carboxylic, phenolic, hydroxyl, and other functional groups.[15,16] There are some reports that covered the electrochemical study of humic-based materials which were also used to fabricate the working electrode for the determination of trace metals in solution.[17,18] In the early 1990s, a report covered the use of anchored Suwanee River HA on a colloidal TiO_2 semiconductor for the reduction of oxazine dye.[19] Recently, HA obtained from soil components was introduced successively as a cathode host

Received: April 9, 2016
Accepted: June 6, 2016
Published: July 6, 2016

DOI: 10.1021/acsomega.6b00010
ACS Omega 2016, 1, 14−18

Scheme 1. Structure of the HA Substance and Its Physical Appearance

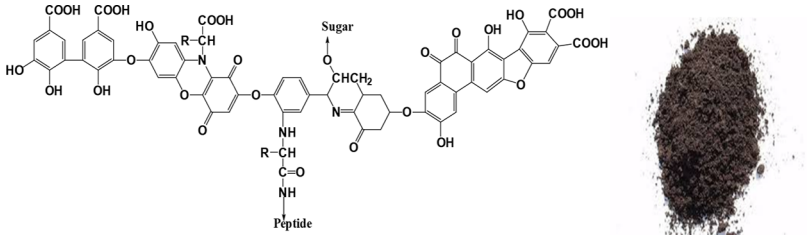

material in lithium ion batteries because of its suitable functionalities.[20]

In this article, a natural polymer, HA with abundant functionalities, is used as a sensitizer in DSSCs. HA shows PCE up to 2.4% with chenodeoxycholic acid (CDCA) as a coadsorbent under illumination of 0.5 sun. The device shows J_{sc} around 6.6 mA/cm^2, 49% incident-photo-to-current conversion efficiency (IPCE), and good stability. Unlike other natural sensitizers, HA shows longer stability and comparative efficiency.

EXPERIMENTAL SECTION

Materials and Methods. HA, ethyl cellulose, α-terpineol, iodine, lithium iodide, 4-*tert*-butyl pyridine, 3-methoxy propionitrile, CDCA, and other required reagents were purchased from Sigma-Aldrich, India, and used as received without further purification. Transparent conducting oxide (TCO) glass and sealing tape were purchased from Solaronix, Switzerland. TiO_2 (P25) particles were purchased from Degussa, Germany. Dimethyl sulfoxide (DMSO) and dimethylformamide (DMF) used in this study were distilled prior to use and stored under molecular sieves. The UV–vis and photoluminescence (PL) spectra of HA were recorded in DMSO/DMF (20:80) using a UV–vis spectrometer (Shimadzu, Japan) and fluorescence spectrophotometer (Ocean Optics, USA), respectively. Electrochemical measurements such as cyclic voltammetry (CV), *I*–*V*, Tafel polarization, and electrochemical impedance spectroscopy (EIS) experiments were carried out using a Solartron electrochemical analyzer (SI 1286). CV was carried out using a three-electrode system in which a Pt disk, Pt wire and nonaqueous Ag/Ag$^+$ served as the working, counter, and reference electrode, respectively, with a $TBAPF_6$ supporting electrolyte at 25 mV/s. However, Tafel polarization data were collected by sweeping the potential from −0.4 to 0.4 V with a scan rate of 20 mV/s, under dark conditions. Photovoltaic characterization (*I*–*V*) of DSSCs was carried out by applying a potential to the device and measuring the generated photocurrent under light illumination of 100 mW/cm^2 using a solar simulator (Photoemission Tech., USA). The IPCE of the devices was recorded using SR 300, Optosolar, Germany, where a 250 W Xe lamp was used as the light source. EIS of devices under dark conditions was measured between 50 Hz and 100 MHz under forward bias. Thermogravimetric analysis (TGA) measurements were carried out using a TGA (SDT Q600, TA Instruments, USA).

DSSC Fabrication. TiO_2 photoelectrodes were prepared on a TCO substrate by a screen-printing technique using titania paste. The paste consists of nanocrystalline TiO_2, ethyl cellulose, and α-terpineol.[21] The TiO_2-coated electrode was calcined in a furnace at 500 °C for 20 min at a heating rate of 4 °C/min. The resultant film has a thickness of around 10 μm. The electrode was allowed to cool up to 80 °C and soaked in a 0.16% (w/v) solution of HA in DMSO/DMF (20:80) for 48 h at 40 °C to ensure complete sensitization. The same process was repeated with additional 0.05 mM CDCA as a coadsorbent in the above composition. The HA-sensitized electrode was washed thoroughly with DMSO and dried under the stream of warm air. A counter electrode was prepared by a spin-coating technique using 50 mM chloroplatinic acid (H_2PtCl_6) solution, followed by calcination at 400 °C for 20 min. DSSCs were assembled in a sandwich-type configuration and sealed using Meltonix hot melt sealing tape (thickness 60 μm). The electrolyte was inserted through the predrilled holes on counter electrodes. The electrolyte consists of 0.5 M LiI, 0.055 M iodine, and 0.5 M 4-*tert*-butyl pyridine in 3-methoxy propionitrile. Holes on the counter electrode were sealed using a cover glass and epoxy adhesive. All cells were stored in a dark place for 24 h prior to photovoltaic measurements.

RESULTS AND DISCUSSION

Photophysical and Electrochemical Properties of HA. The UV–vis absorption spectra (Figure 1a) of 0.16% (w/v)

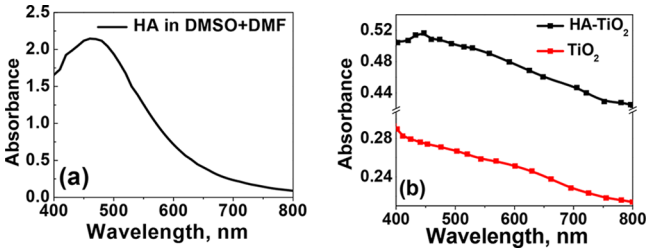

Figure 1. UV–vis absorption spectra of (a) pure HA in DMSO/DMF and (b) an HA-loaded TiO_2 film.

HA in DMSO/DMF were measured, and the corresponding optical parameters are listed in Table 1. The spectra cover a maximum visible range because of their blackish brown color (Scheme 1) with maximum absorbance at 461 nm. The UV–vis absorbance spectra of the dye-loaded TiO_2 (Figure S1) are shown in Figure 1b. A slight hypsochromic shift of 12 nm was noticed for the absorption maxima of the dye-loaded TiO_2 film in comparison with that of the dye solution. This hypsochromic

Table 1. Photophysical and Electrochemical Parameters of HA

dye	λ_{obs} [a] (nm)	ε [a] (M^{-1} cm^{-1})	E_g [b] (eV)	E°_{onset} [c] vs Fc/Fc$^+$ (V)	HOMO [c] (V)	LUMO [d] (V)
HA	461	16 002	1.97	0.007	0.637	−1.330

[a]Measured in DMSO/DMF (20:80). [b]Measured from λ_{onset}. [c]All potentials were obtained from the CV. Potentials measured vs Fc/Fc$^+$ were converted to NHE by addition of +0.63 V (ref 25). [d]Calculated from LUMO = HOMO − E_g.

DOI: 10.1021/acsomega.6b00010
ACS Omega 2016, 1, 14–18

shift of the absorbance maxima is because of the deprotonation effect when HA was anchored to the nanocrystalline TiO_2 film.[22]

In addition, the amount of HA adsorbed on titania (area = 1 cm^2) was measured by performing a desorption study in the presence of aqueous NaOH. The UV−vis absorbance spectra before and after desorption are given in Figure S2. From this figure it is revealed that 0.02% (w/v) HA adsorbed on the titania surface from the 0.16 % (w/v) dye bath. Hence, it is confirmed that the presence of a good number of anchoring groups is responsible for HA loading on the titania surface. Reports are also available that explain the detailed structure of HA using Fourier transform infrared (FTIR) spectroscopy and confirmed the presence of a large number of chemically reactive oxygen groups, including carboxyl, phenolic, and alcoholic hydroxyl groups in HA.[20]

The PL spectra of 0.16% (w/v) HA in DMSO/DMF are given in Figure 2. HA exhibits maximum emission at 550 nm

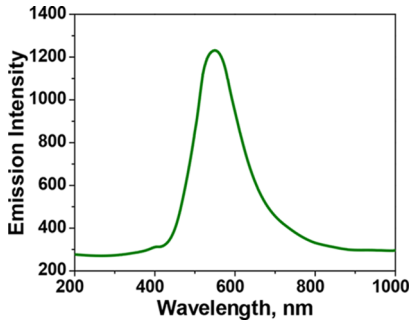

Figure 2. PL emission spectra of HA in DMSO/DMF (20:80).

and tailing up to 800 nm with an excitation wavelength of 405 nm. Absorption and emission in the visible spectrum are associated with conjugated unsaturated systems such as quinonoid-type cyclic aromatic hydrocarbons with highly substituted carbonyl (C═O) and carboxylic groups. Senesi et al. also reported a similar kind of observation in the case of naturally extracted humic as well as fulvic acid.[23,24]

Electrochemical properties of HA were measured by a CV study with a three-electrode system in DMSO/DMF solution at 0.16% (w/v) concentration with ferrocene/ferrocenium (Fc/Fc^+) as the internal reference (Figure 3), and the resultant data are listed in Table 1. The observed quasi-reversible redox wave can be attributed to the oxidation of the aromatic-conjugated quinonoid portion of the HA component. HA exhibits clear oxidation and reduction peaks compared with other natural sensitizers, which reflects a more electron-rich nature of HA. Hence, it shows an absorbance band at longer wavelengths in

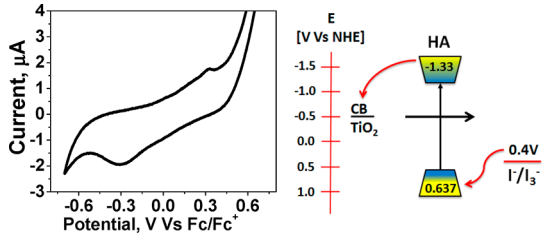

Figure 3. Cyclic voltammogram (CV) of HA in DMSO/DMF with Pt as a working electrode (on left) and energy-level diagram of HA relevant to the DSSC (on right).

UV−vis spectra. This gives an appropriate band gap with the lowest unoccupied molecular orbital (LUMO) level above the conduction band of TiO_2 and highest occupied molecular orbital (HOMO) level below the redox potential of the I^-/I_3^- redox couple, which facilitates effective charge injection and dye regeneration, respectively (energy-level diagram in Figure 3).

The thermal stability of HA was tested by thermogravimetric analysis (Figure S3), and it found that HA is stable up to 300 °C.

Characterization of DSSCs. Photocurrent-density−voltage ($I-V$) plots of the devices under illumination of 0.1, 0.5, and 1 sun are shown in Figure 4a. Additionally, dark current-density−

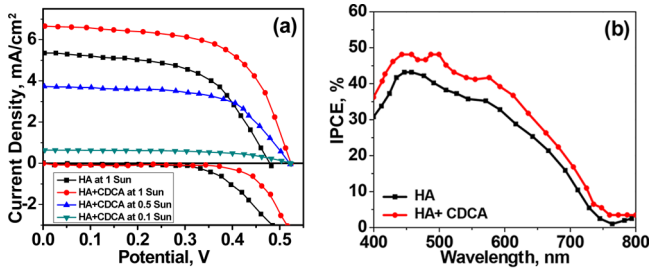

Figure 4. (a) $J-V$ curves and (b) IPCE of DSSCs based on the HA and with CDCA.

voltage curves of HA-based DSSC devices with and without CDCA are also depicted in the figure. The figure reveals the remarkable difference in the performance of devices sensitized with HA and coadsorbed with CDCA. The photovoltaic parameters such as open circuit voltage (V_{oc}), short-circuit current (J_{sc}), fill factor (FF), and PCE (η) were deduced from these curves and are summarized in Table 2.

The DSSC sensitized with HA produced J_{sc} = 5.3 mA/cm^2, V_{oc} = 0.472 V, and FF = 56.6% corresponding to a PCE of 1.4%. The data reveal that HA itself is efficient as a sensitizer in the DSSC and the entity responsible for binding in HA is considered to be quinine and/or carboxylic acid groups. The PCE was further improved to 2.1% (J_{sc} = 6.6 mA/cm^2, V_{oc} = 0.524 V, and FF = 60.7%) using the coadsorbent, CDCA, under 100 mW/cm^2 (1 sun) illumination. The same device delivered 2.4% PCE under 50 mW/cm^2 illumination. A remarkable difference in photovoltaic characteristics was observed in both the devices because of the coadsorbed effect.[2,26−28] The large and imbalanced structure of HA faces the problem of aggregation and empty loops on the TiO_2 surface. CDCA may alleviate dye aggregation and suppresses the dark current as well as internal quenching of the excited dye molecules. This combined effect of CDCA enhances the performance of the HA device. The IPCE spectra of DSSCs are shown in Figure 4b. The HA + CDCA device gives a higher IPCE value (49%) than the pristine HA device. HA shows a good value of IPCE at ∼449 nm, which indicates that it has a very efficient acceptor or anchoring group. The higher IPCE value of the HA + CDCA-sensitized device, compared with that of HA, indicates an enhancement in the photocurrent because of the filling of small gaps between HA molecules by CDCA.

Further insights into the electron transfer kinetics of these DSSCs were obtained using electrochemical impedance spectroscopy and the Tafel polarization technique. A typical Nyquist plot of the DSSC device consists of three semicircles in a complex plane.[29] The response of the AC signal is fitted using

DOI: 10.1021/acsomega.6b00010
ACS Omega 2016, 1, 14−18

Table 2. $J-V$ Parameters of HA and HA + CDCA Devices under Different Light Intensities

dye	P_{in} (mW cm^{-2})	J_{sc} (mA cm^{-2})	V_{oc} (V)	FF (%)	PCE (%)
HA	100	5.3 ± 0.3	0.472 ± 0.010	56.6 ± 0.5	1.4 ± 0.1
HA + CDCA	100	6.6 ± 0.7	0.524 ± 0.021	60.7 ± 0.7	2.1 ± 0.1
HA + CDCA	50	3.7 ± 0.5	0.522 ± 0.020	60.8 ± 0.5	2.4 ± 0.1
HA + CDCA	10	0.6 ± 0.4	0.520 ± 0.020	58.6 ± 0.5	2.0 ± 0.1

an appropriate equivalent-circuit model to extract the desired parameters of electron transfer reactions.

The impedance response of the first depressed semicircle was fitted using a parallel resistor–capacitor (RC) circuit (inset of Figure 5a) to estimate the charge transfer resistance. The

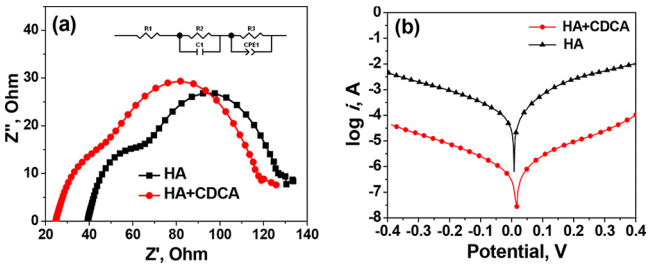

Figure 5. (a) Electrochemical impedance response recorded in the dark under forward bias and (b) Tafel polarization curves of DSSCs.

observed values of R_{ct} are 25 and 39 Ω for the device with HA + CDCA and HA, respectively. This suggests smooth catalytic reactions at the Pt counter electrode. It can be seen from the graph that the second arc is smaller in the case of the HA + CDCA-based device, confirming a better charge injection than the corresponding HA device. Further insight was obtained by the Tafel polarization technique, which shows the kinetics of the reaction in the electrolyte component of the dye solar cell under dark conditions (Figure 5b).[30,31] The well-known Butler–Volmer equation (eq 1) was used to fit the Tafel polarization curves that give information about rates of cathodic and anodic reactions occurring at the semiconductor/electrolyte interface

$$J = -J_0\left[\exp\frac{\alpha_c nF}{RT}(E - E_{eq}) - \exp\frac{\alpha_a nF}{RT}(E - E_{eq})\right] \quad (1)$$

where J_0 is the exchange current density, E is the applied voltage, E_{eq} is the equilibrium potential of the I^-/I_3^- redox system, and α_a and α_c are the anodic and cathodic transfer coefficients, respectively. It is clear from this equation that $J = J_0$ as $E = E_{eq}$ in the dark. Exchange current densities for all of the DSSCs were estimated by fitting the Tafel plot with Corrview software and found to be 1.0 and 0.025 μA for HA and HA + CDCA, respectively. The intensity of the dark current is directly related to the back electron transfer from the TiO_2 matrix to the electrolyte component. Moreover, the higher dark current would lead to the lower open circuit voltage because of the recombination of electrons. This fact agrees well with the V_{oc} obtained from Figure 4, which shows the highest PCE value for the HA + CDCA-based device resulting from lower recombination. All remaining devices exhibited similar results as obtained from photovoltaic measurements.

Figure 6 covers the stability of the best-performing HA DSSC devices with and without CDCA. No appreciable degradation was noticed in all photovoltaic parameters under illumination of 1 sun for 1000 h. Hence, HA-based devices

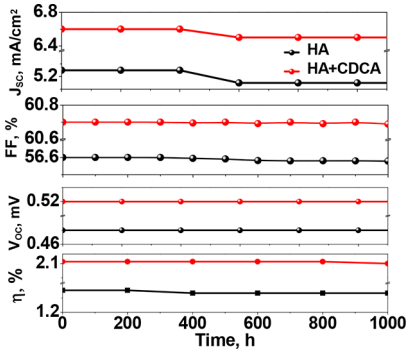

Figure 6. Photovoltaic parameters of devices measured under illumination of 1 sun for 1000 h.

unveiled considerable efficiency and excellent long-term photostability.

CONCLUSIONS

HA, a natural polymer, has a photoresponsive character and covers a broad spectrum of the visible region. The abundance of functionalities in the framework of HA allows it to anchor onto the titania surface, which has been successfully employed as a thermally stable natural light harvesting agent. The DSSC device sensitized with HA showed 1.4% PCE under illumination of 1 sun. An enhancement in PCE (2.1%) was noticed when CDCA was used as a coadsorbent. An optimum 2.4% PCE was achieved for the same device under illumination of 0.5 sun. The said efficiency was good compared with that of other reported natural sensitizers. Further, the modification in the structure of multifunctionalities of HA may lead to an enhancement in efficiency. Hence, this work will pave the way for utilizing soil components for the generation of energy from sunlight.

ASSOCIATED CONTENT

Supporting Information

The Supporting Information is available free of charge on the ACS Publications website at DOI: 10.1021/acsomega.6b00010.

Photographs of the photoanode before and after sensitization, details of the dye adsorption and desorption study along with UV–vis spectra, and thermogravimetric analysis of HA (PDF)

AUTHOR INFORMATION

Corresponding Author

*E-mail: soni_b21@yahoo.co.in.

Notes

The authors declare no competing financial interest.

ACKNOWLEDGMENTS

This work has been financially supported by the Science and Engineering Research Board (SERB), New Delhi, India, under

DOI: 10.1021/acsomega.6b00010
ACS Omega 2016, 1, 14–18

grant no. SB/FT/CS-173/2011. The authors are also thankful to the Head, Department of Chemistry, Sardar Patel University for providing basic amenities for carrying out this work.

REFERENCES

(1) O'Regan, B.; Grätzel, M. A low-cost, high-efficiency solar cell based on dye-sensitized colloidal TiO_2 films. *Nature* **1991**, *353*, 737−740.
(2) Papageorgiou, N. *Dye-Sensitized Solar Cells Rival Conventional Cell Efficiency*; Ecole Polytechnique Federale de Lausanne (EPFL), News Mediacom, 2015. http://actu.epfl.ch/news/dye-sensitized-solar-cells-rival-conventional-ce-2/.
(3) Urbani, M.; Grätzel, M.; Nazeeruddin, M. K.; Torres, T. Meso-Substituted Porphyrins for Dye-Sensitized Solar Cells. *Chem. Rev.* **2014**, *114*, 12330−12396.
(4) Nazeeruddin, M. K.; Péchy, P.; Liska, P.; Renouard, T.; Zakeeruddin, S. M.; Humphry-Baker, R.; Comte, P.; Cevey, L.; Costa, E.; Shklover, V.; Spiccia, L.; Deacon, G. B.; Bignozzi, C. A.; Gratzel, M. Engineering of Efficient Panchromatic Sensitizers for Nanocrystalline TiO_2-Based Solar Cells. *J. Am. Chem. Soc.* **2001**, *123*, 1613−1624.
(5) Argazzi, R.; Larramona, G.; Contado, C.; Bignozzi, C. A. Preparation and photoelectrochemical characterization of a red sensitive osmium complex containing 4,4′,4″-tricarboxy-2,2′:6′,2″-terpyridine and cyanide ligands. *J. Photochem. Photobiol. A* **2004**, *164*, 15−21.
(6) Mishra, A.; Fischer, M. K. R.; Bäuerle, P. Metal-free organic dyes for dye-sensitized solar cells: from structure: property relationships to design rules. *Angew. Chem., Int. Ed.* **2009**, *48*, 2474−2499.
(7) Soni, S. S.; Fadadu, K. B.; Vaghasiya, J. V.; Solanki, B. G.; Sonigara, K. K.; Singh, A.; Das, D.; Iyer, P. K. Improved molecular architecture of D−π−A carbazole dyes: 9% PCE with a cobalt redox shuttle in dye sensitized solar cells. *J. Mater. Chem. A.* **2015**, *3*, 21664−21671.
(8) Kay, A.; Graetzel, M. Photosensitization of TiO_2 Solar Cells with Chlorophyll Derivatives and Related Natural Porphyrins. *J. Phys. Chem.* **1993**, *97*, 6272−6277.
(9) Calogero, G.; Di Marco, G.; Cazzanti, S.; Caramori, S.; Argazzi, R.; Di Carlo, A.; Bignozzi, C. A. Efficient Dye-Sensitized Solar Cells Using Red Turnip and Purple Wild Sicilian Prickly Pear Fruits. *Int. J. Mol. Sci.* **2010**, *11*, 254−267.
(10) Calogero, G.; Bartolotta, A.; Di Marco, G.; Di Carlob, A.; Bonaccorso, F. Vegetable-based dye-sensitized solar cells. *Chem. Soc. Rev.* **2015**, *44*, 3244−3294.
(11) Stevenson, F. J. *Humus Chemistry: Genesis, Composition, Reactions*; John Wiley & Sons: New York, 1994; pp 285−302.
(12) Ghabbour, E. A.; Davies, G. *Humic Substances: Structures, Models and Functions*; RSC Publishing: Cambridge, U.K., 2001; pp 19−30.
(13) Senesi, N.; Loffredo, E. The chemistry of soil organic matter. In *Soil Physical Chemistry*, 2nd ed.; Sparks, D. L., Ed.; CRC Press: Boca Raton, 1999; Chapter 6, pp 239−370.
(14) Zara, L. F.; Rosa, A. H.; Toscano, I. A. S.; Rocha, J. C. A Structural Conformation Study of Aquatic Humic Acid. *J. Braz. Chem. Soc.* **2006**, *17*, 1014−1019.
(15) Oviasogie, P. O.; Aisueni, N. O. Selected spectroscopic characteristics of humic acid from compost and soil supporting oil palm. *Inter J. Chem.* **2004**, *14*, 78−85.
(16) Kantar, C.; Karadagli, F. Comparison of Two Methods for the Determination of Stability Constants for Metal-NOM Interactions. *Turkish J. Eng. Environ. Sci.* **2005**, *29*, 297−308.
(17) Aeschbacher, M.; Sander, M.; Schwarzenbach, R. P. Novel electrochemical approach to assess the redox properties of humic substances. *Environ. Sci. Technol.* **2010**, *44*, 87−93.
(18) Wang, C.; Zhang, H.; Sun, Y.; Li, H. Electrochemical behaviour and determination of gold at chemically modified carbon past electrode by the ethylenediamine fixed humic acid preparation. *Anal. Chim. Acta* **1998**, *361*, 133−139.
(19) Vinodgopal, K. Environmental photochemistry: electron transfer from excited humic acid to TiO_2 colloids and semiconductor mediated reduction of oxazine dyes by humic acid. *Res. Chem. Intermed.* **1994**, *20*, 825−833.
(20) Zhu, H.; Yin, J.; Zhao, X.; Wang, C.; Yang, X. Humic acid as promising organic anodes for lithium/sodium ion batteries. *Chem. Commun.* **2015**, *51*, 14708−14711.
(21) Fadadu, K. B.; Soni, S. S. Spectral sensitization of TiO_2 by new hemicyanine dyes in dye solar cell yielding enhanced photovoltage: Probing chain length effect on performance. *Electrochim. Acta* **2013**, *88*, 270−277.
(22) Zhu, W.; Wu, Y.; Wang, S.; Li, W.; Li, X.; Chen, J.; Wang, Z.-S.; Tian, H. Organic D-A-π-A Solar Cell Sensitizers with Improved Stability and Spectral Response. *Adv. Funct. Mater.* **2010**, *21*, 756−763.
(23) Senesi, N.; Miano, T. M.; Provenzano, M. R.; Brunetti, G. Characterization, Differentiation, and Classification of Humic Substances by Fluorescence Spectroscopy. *Soil Sci.* **1991**, *152*, 259−271.
(24) Senesi, N.; D'Orazio, V.; Ricca, G. Humic Acids in the First Generation of EUROSOILS. *Geoderma* **2003**, *116*, 325−344.
(25) Pavlishchuk, V. V.; Addison, A. W. Conversion Constants for Redox Potentials Measured vs. Different Reference Electrodes in Acetonitrile Solutions at 25 °C. *Inorg. Chim. Acta* **2000**, *298*, 97−102.
(26) Xie, Y.; Tang, Y.; Wu, W.; Wang, Y.; Liu, J.; Li, X.; Tian, H.; Zhu, W. H. Porphyrin Cosensitization for a Photovoltaic Efficiency of 11.5%: A Record for Non-Ruthenium Solar Cells Based on Iodine Electrolyte. *J. Am. Chem. Soc.* **2015**, *137*, 14055−14058.
(27) Sun, X.; Wang, Y.; Li, X.; Ågren, H.; Zhu, W.; Tian, H.; Xie, Y. Cosensitizers for simultaneous filling up of both absorption valleys of porphyrins: a novel approach for developing efficient panchromatic dye-sensitized solar cells. *Chem. Commun.* **2014**, *50*, 15609−15612.
(28) Wang, Y.; Chen, B.; Wu, W.; Li, X.; Zhu, W.; Tian, H.; Xie, Y. Efficient Solar Cells Sensitized by Porphyrins with an Extended Conjugation Framework and a Carbazole Donor: From Molecular Design to Cosensitization. *Angew. Chem., Int. Ed.* **2014**, *53*, 10779−10783.
(29) Adachi, M.; Sakamoto, M.; Jiu, J.; Ogata, Y.; Isoda, S. Determination of Parameters of Electron Transport in Dye-Sensitized Solar Cells Using Electrochemical Impedance Spectroscopy. *J. Phys. Chem. B* **2006**, *110*, 13872−13880.
(30) Zhang, C.; Dai, J.; Huo, Z.; Pan, X.; Hu, L.; Kong, F.; Huang, Y.; Sui, Y.; Fang, X.; Wang, K.; Dai, S. Influence of 1-methylbenzimidazole interactions with Li^+ and TiO_2 on the performance of dye-sensitized solar cells. *Electrochim. Acta* **2008**, *53*, 5503−5508.
(31) Cameron, P. J.; Peter, L. M.; Hore, S. How important is the back reaction of electrons via the substrate in dye-sensitized nanocrystalline solar cells? *J. Phys. Chem. B* **2005**, *109*, 930−936.

DOI: 10.1021/acsomega.6b00010
ACS Omega 2016, 1, 14−18